Macromolecules

pubs.acs.org/Macromolecules Article

Accelerated and Controlled Polymerization of Tryptophan *N*-Carboxyanhydride

Chenlin Ji, Tingting Cao, Luyao Wang, Zhuohang Zhou, Yu Zhao, Xingliang Liu, Chengjie Sun,* Ziyuan Song,* and Jianjun Cheng*

Cite This: *Macromolecules* 2026, 59, 6854−6863 Read Online

ACCESS | Metrics & More | Article Recommendations | Supporting Information

ABSTRACT: Tryptophan (Trp or W) was distinguished among eukaryotic amino acids due to its unique physicochemical properties, enabling diverse applications in biomedical research. However, synthesizing well-defined, high-molecular-weight poly(L-tryptophan) (PLW) via controlled ring-opening polymerization (ROP) of L-tryptophan *N*-carboxyanhydride (Trp-NCA) remains challenging, primarily due to slow kinetics and interference of the secondary structure. In this work, we present a synergistic organic acid−base catalytic strategy to overcome these obstacles. The organic base disrupts the inhibitory indole−amine interactions, thereby accelerating the polymerization, while the organic acid mitigates uncontrolled two-stage polymerization kinetics by eliminating the initial lag phase. This approach enables well-controlled ROP of NCAs that exhibits features of a living polymerization, thus achieving precise synthesis of PLW homopolymers and Trp-rich copolypeptides with predictable molecular weights (MWs), narrow dispersity ($Đ$ < 1.20), and different segment structures. Appealing MW-dependent secondary structures and Trp content-dependent fluorescence properties were characterized based on these polypeptides. This strategy provides an efficient route to Trp-containing polypeptides, expanding their utility in protein mimicking and functional biomaterials.

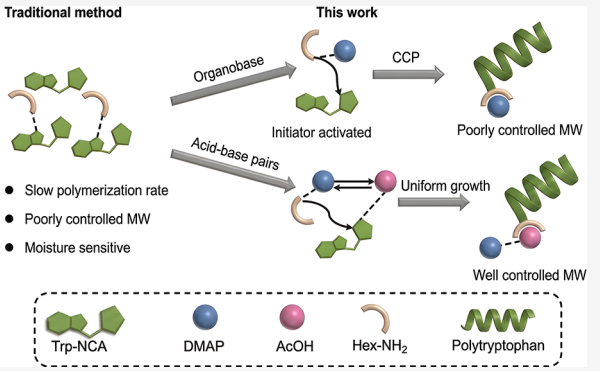

INTRODUCTION

Tryptophan (Trp or W), among the naturally encoded eukaryotic amino acids, stands out by its distinctive physicochemical properties.[1−5] The unique chemical activity of tryptophan primarily arises from its indole side chain, which engages in a broad range of noncovalent interactions, such as cation−π, $\pi-\pi$ stacking, and hydrophobic interactions.[1−5] These interactions make Trp−Trp pairs a paradigmatic model for the design of molecules with stable secondary structures, exemplified by the well-known "Trpzip" peptides.[6,7] In the context of materials science, poly(L-tryptophan) (PLW)-based materials have attracted significant attention owing to their excellent gelation ability,[6,8−11] fluorescent activity,[12,13] charge-transfer capability,[14,15] and photocatalytic capability.[16,17]

Despite these properties, the studies on tryptophan-based materials were hindered by the difficulties in synthesizing well-defined, high molecular-weight (MW) PLW and its derivatives. Specifically, the ring-opening polymerization (ROP) α-amino acid *N*-carboxyanhydrides (NCAs), one of the most versatile approaches to prepare polypeptides,[18−22] was not well studied for Trp-NCA.[23−26] As an important alternative to NCA ring-opening polymerization, the *N*-phenoxycarbonyl (NPC) amino acid approach has enabled the preparation of well-defined polypeptide materials, including PLW with uniform end groups.[23] Nevertheless, the reaction still required several days to reach completion, even in the presence of acid catalysts.[24] Other NCA polymerization methods are often limited by slow kinetics or the requirement for a strict inert-gas atmosphere.[25−28] Considering the recent advances in NCA and polypeptide chemistry,[29−38] it is of great interest to study the synthesis, characterization, and photophysical properties of tryptophan-based polypeptide materials, enriching the toolbox for the design of functional polypeptide materials.

In this work, we developed an organic acid−base cooperative strategy for the controlled ROP of Trp-NCA (Scheme 1), establishing a robust platform for the synthesis of PLW and its copolypeptide analogues with precise MW control and narrow dispersity. While organic bases like 4-dimethylpyridine (DMAP) accelerated the polymerization rate, acetic acids helped improve the MW control. A series of PLW and its copolypeptide analogues were thus successfully prepared in a

Received: February 12, 2026
Revised: May 13, 2026
Accepted: May 17, 2026
Published: June 1, 2026

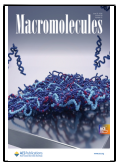

https://doi.org/10.1021/acs.macromol.6c00471
Macromolecules 2026, 59, 6854−6863

Scheme 1. Illustration of Conventional Trp-NCA Polymerization with Traditional Method and the Polymerization in This Work in the Presence of Organic Acids and DMAP

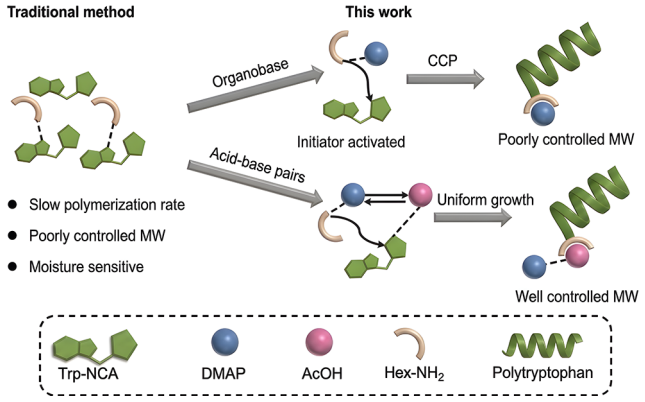

controlled and efficient manner, which exhibited tryptophan-content-dependent assembly behaviors and fluorescent properties. We believe that this work provides a robust strategy for accessing tryptophan-containing polypeptides and offers new opportunities for protein mimicking and biomimetic materials.

RESULTS AND DISCUSSION

Slow Polymerization Kinetics of Trp-NCA Due to Side-Chain Indoles

To study the incorporation of tryptophan units into polypeptides, L-tryptophan NCA (Trp-NCA) was first prepared and purified, whose molecular structure was confirmed by nuclear magnetic resonance spectroscopy (NMR) and X-ray diffraction (XRD). The polymerization of Trp-NCA was first initiated by *n*-hexylamine (Hex-NH_2) in a cosolvent containing *N*,*N*-dimethylformamide (DMF) and dichloromethane (DCM) ($[M]_0/[I]_0 = 50$, $[M]_0 = 0.2$ M) (Figure 1a). The cosolvent was used to combine the advantages of DMF and DCM, which balanced the polymer solubility as well as the polymerization rate, yielding polypeptides in an accelerated and controlled manner.[39] Nevertheless, the polymerization proceeded slowly that the monomer conversion was only ~20% after 8 h from FTIR analysis (Figures 1b and S1). In contrast, the polymerization of γ-benzyl-L-glutamate NCA (BLG-NCA), one of the most commonly studied NCA monomers, exhibited >95% conversion within 1 h under identical conditions, suggesting the slow polymerization kinetics of Trp-NCA monomers. While primary amine-initiated homopolymerization or copolymerization of Trp-NCA was reported in conventional solvents like DMF,[10,25] only few works indicated their slower kinetics compared to other NCA monomers in unconventional solvents like acetonitrile or dichloroethane.[40] The chlorine content in purified Trp-NCA was below the detection limit, ruling out the

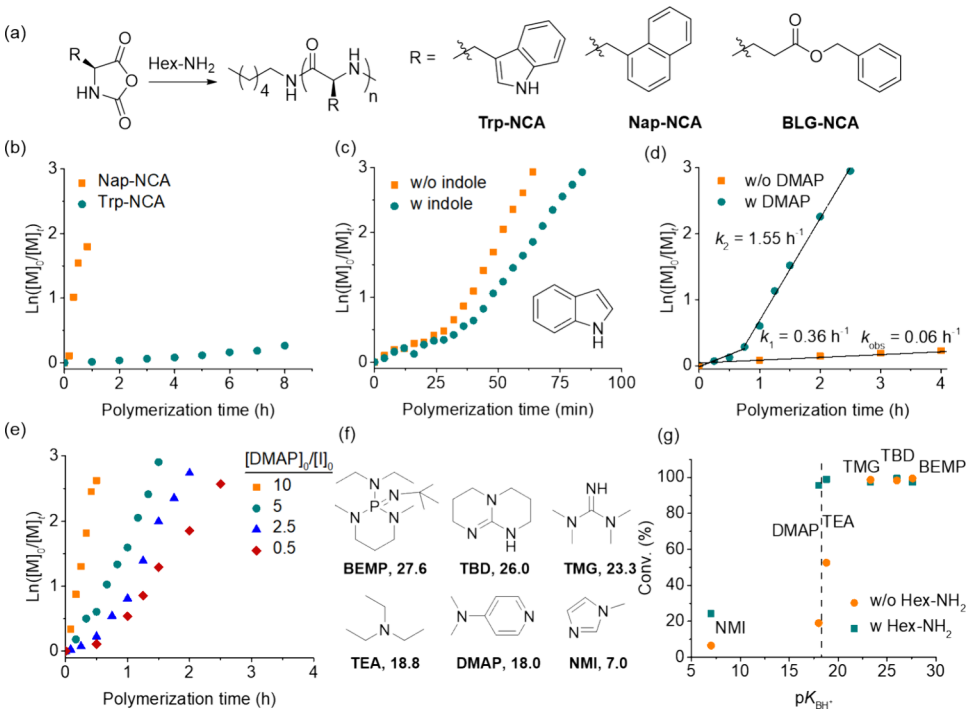

Figure 1. Impact of indole side chain on the polymerization behaviors. (a) Synthetic route to PLW through ring-opening polymerization of Trp-NCA. The polymerization of Nap-NCA and BLG-NCA was used as control. (b) Semilogarithmic kinetic plot of polymerization of Trp-NCA or Nap-NCA. (c) Semilogarithmic kinetic plot of polymerization of BLG-NCA in DCM in the presence or absorbance of indole. $[M]_0/[indole]_0 = 1$. (d) Semilogarithmic kinetic plot of polymerization of Trp-NCA in DMF/DCM initiated by Hex-NH_2 in the presence or absences of DMAP. $[DMAP]_0/[I]_0 = 1$. (e) Semilogarithmic kinetic plot of polymerization of Trp-NCA in DMF/DCM initiated by Hex-NH_2 at various $[DMAP]_0/[I]_0$. (f) Chemical structures of various organic bases with different pK_{BH+} values. (g) The plot of the 3 h NCA conversion against the pK_{BH+} value of added organic bases in the presence or absence of Hex-NH_2. $[base]_0/[I]_0 = 1$. All polymerizations were conducted in DMF/DCM (1:1, v/v) with Hex-NH_2 as the initiator. $[M]_0/[I]_0 = 50$, $[M]_0 = 0.2$ M.

https://doi.org/10.1021/acs.macromol.6c00471
Macromolecules 2026, 59, 6854−6863

possibility that the slow kinetics originated from the existence of excessive HCl or phosgene impurities.

Inspired by the recent reports on the catalytic roles of indole N−H groups during the ROP of lactones,[41] The side-chain indole of Trp-NCA appeared to be responsible for the slowing polymerization progress. To validate our hypothesis, 1-naphthylalanine NCA (Nap-NCA) was prepared and purified as a control monomer (Figure 1a), whose polymerization proceeded rapidly, achieving a monomer conversion of 83% within 50 min (Figure 1b). Further polymerization led to the precipitation of resulting polypeptides. In the absence of heterocycle N−H moiety on the side chains of Trp-NCA, the consumption of Nap-NCA was comparable with that of BLG-NCA, highlighting the unique role of indole moiety in mediating slower polymerization kinetics. Meanwhile, BLG-NCA was polymerized in the presence of equimolar indole in DCM, which took 20 min longer to complete compared to that without indole (Figure 1c). Even though the indole molecule was spatially separated with the five-membered ring of NCA (i.e., less neighboring effect), the polymerization was still slowed down, confirming the modulation of kinetic profiles by side-chain indole groups. While the detailed mechanism is not clear at this moment, the weak acidity and the large bicyclic π-conjugation system of indole likely mediated the interaction with propagating amino groups that weakened their nucleophilicity slowing down the kinetics.[42] NMR characterization revealed the upfield shifts of indole N−H and adjacent C−H protons upon the ring-opening, suggesting that the N−H likely participated into certain interactions with the primary amine groups (Figure S2). To further probe the reactivity difference between Trp-NCA and BLG-NCA, DFT calculations were performed using model reactions with ethylamine. Single-point energies were calculated at the B3LYP-D3BJ/def2-TZVP/PCM (DMF/DCM = 1:1) level to construct the Gibbs free energy profiles. The calculations showed that nucleophilic addition of ethylamine to the NCA monomer is the key rate-determining step in both systems. For Trp-NCA, the barrier associated with TS1 relative to INT1 is 41.33 kcal/mol, whereas the corresponding barrier for BLG-NCA is lower at 40.48 kcal/mol (Figure S2). This higher activation barrier is consistent with the experimental observation, suggesting that the indole-containing side chain contributes to the reduced polymerization reactivity.

With the slow kinetics, the polymerization of Trp-NCA was vulnerable to various side reactions, such as water-initiated NCA degradation. Matrix-assisted laser desorption/ionization time-of-flight (MALDI-TOF) mass spectra revealed multiple polymeric species when Trp-NCA was exposed under ambient conditions, which was attributed to water-initiated side reactions and self-polymerization (Figure S3). After a 48 h polymerization of Trp-NCA initiated by Hex-NH_2, on the other hand, the obtained MW of resulting PLW (i.e., 20.0 kDa) was much larger than the theoretical value calculated from $[M]_0/[I]_0$ (i.e., 9.4 kDa) (Figure S4). The dRi signal indicated that chain growth during Trp-NCA polymerization was not uniform, as oligomeric peaks were clearly observed throughout the polymerization process (Figure S4). In contrast, an improved MW was observed when the polymerization was conducted at 4 °C with suppressed side reactions (Table S1). Nevertheless, the even longer polymerization time (i.e., 72 h) at a low temperature validated the necessity to design accelerated polymerization systems for Trp-NCA.

Accelerated Polymerization of Trp-NCA Catalyzed by Organic Bases

While the reason for the inhibitory effect of side-chain indoles was not clear at the moment, we sought to neutralize their negative impact on the kinetics through the addition of catalysts. Organic bases were selected because they can competitively interact with the side-chain indole groups of Trp-NCA and thus reactivate the propagating amino groups. Specifically, DMAP was added into the polymerization solution at $[DMAP]_0/[I]_0$ = 1, which significantly boosted the polymerization of Trp-NCA that >95% monomer was consumed within 3 h at $[M]_0/[I]_0 = 50$ (Figure 1d and Figure S1). On the other hand, other reported catalysts for NCA polymerization, including crown ether (CE),[39,43] organic acid,[44−48] and thiourea,[49,50] did not exhibit obvious accelerating effect, highlighting the unique role of DMAP (Figure S5 and Table S2). Although the acid-catalyzed system displays one-stage kinetics and a unimodal GPC profile, the slow reaction rate may allow competing hydrolysis of Trp-NCA to become more pronounced (Figure S5). Additionally, while the increase in $[DMAP]_0/[I]_0$ further accelerated the polymerization (Figure 1e), obvious shoulder peaks were observed on gel permeation chromatography (GPC) traces (Figure S6), which were attributed to multiple polymerization pathways. Monomodal GPC peaks were only observed when $[DMAP]_0/[I]_0 \leq 2.5$. Because DMAP could act as a conventional basic initiator that polymerizes NCA through an activated monomer mechanism (AMM), boosting $[DMAP]_0/[I]_0$ might lead to the uncontrolled polymerization from both Hex-NH_2 and DMAP. Meanwhile, the polymerization was much slower in the absence of Hex-NH_2, exhibiting ∼17% monomer conversion in 3 h with only oligomers (Figure S6). Mechanistic studies suggest that DMAP perturbed the local environment of Hex-NH_2 *via* hydrogen-bond interactions, thereby enhancing its reactivity for the accelerated ring-opening reactions (Figure S6). Meanwhile, NMR titration further revealed weak interactions between the NCA ring and DMAP (Figure S7), suggesting that the primary role of DMAP was to activate the initiator and propagating chain-ends. As a result, DMAP likely served like a kinetic catalyst rather than a basic initiator or scavenger (i.e., to clean up acidic impurities) at low $[DMAP]_0/[I]_0$ in our system. Moreover, MALDI-TOF MS analysis suggested that the C termini of resulting PLW were indeed *n*-hexyl groups at $[DMAP]_0/[I]_0$ = 1 (Figure S7), validating that the polymerization proceeded with the normal amine mechanism (NAM). The similar kinetic role of organic bases as catalysts rather than initiators was also reported during NCA polymerization.[51−54]

Besides DMAP, the catalytic effects of other organic bases were also explored, aiming to further study the catalytic mechanism (Figure 1f). The addition of stronger bases than DMAP (the pK_a of conjugated acid in acetonitrile, pK_{BH^+} = 18.0),[54−57] like 1,3-dimethyl-2-(diethylamino)-2-(*tert*-butylimino)hexahydro-1,3,2-diazaphosphorine (BEMP, pK_{BH^+} = 27.6), led to fast consumption of Trp-NCA even in the absence of Hex-NH_2, indicating a polymerization with an AMM mechanism (Figure S8). The use of weaker bases like *N*-methylimidazole(NMI,pK_{BH^+} = 7.0), however, resulted in unsubstantial rate acceleration (Figure S8). By plotting the differences of the conversion of Trp-NCA after 3-h polymerization in the presence and absence of Hex-NH_2 against the pK_{BH^+} ($[M]_0/[I]_0 = 50$, $[M]_0$ = 0.2 M), we showed the ability of organic bases to catalyze the polymerization of Trp-NCA while maintaining minimal AMM initiation (Figure 1g). Notably, DMAP outperformed other bases with >90% monomer

https://doi.org/10.1021/acs.macromol.6c00471
Macromolecules 2026, 59, 6854−6863

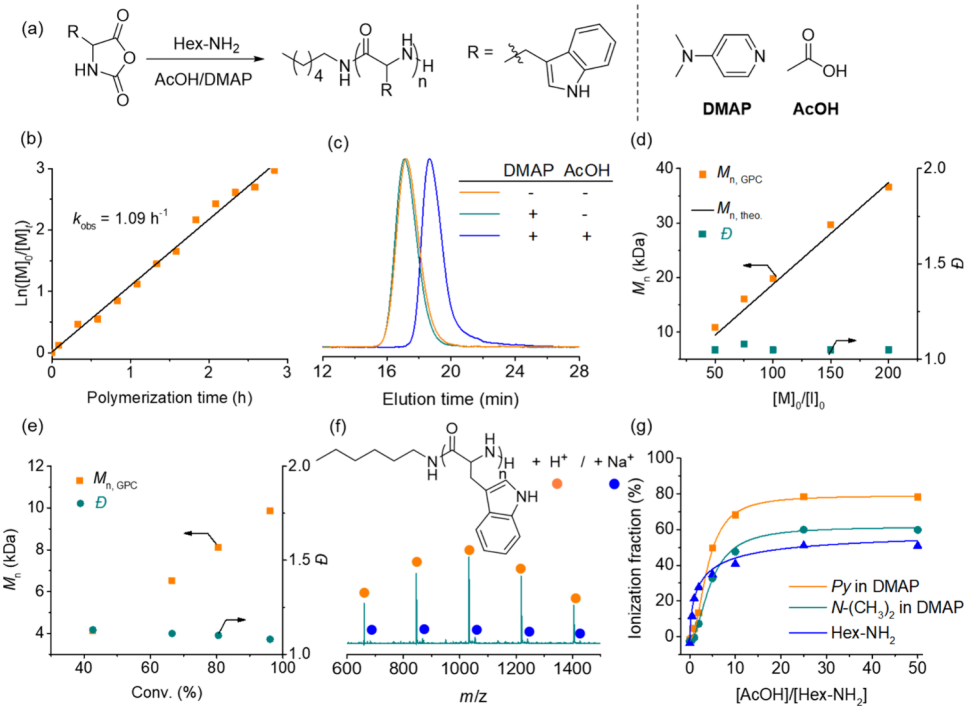

Figure 2. AcOH/DMAP mediated the living polymerization of Trp-NCA. (a) Synthetic route to PLW in the presence of AcOH and DMAP. (b) Semilogarithmic kinetic plot of polymerization of Trp-NCA in the presence AcOH/DMAP. (c) Normalized GPC-LS trace of polymerization of Trp-NCA in the presence and absence of AcOH or DMAP. (d) MWs and dispersity of PLW obtained from polymerization of Trp-NCA at various $[M]_0/[I]_0$ ratios. (e) M_n−conversion plot of the polymerization of Trp-NCA in the presence of AcOH/DMAP. (f) MALDI-TOF result and chemical structures of the resulting PLW at $[M]_0/[I]_0 = 5$. (g) The ionization fraction of Hex-NH_2 and DMAP in the presence of AcOH at various $[AcOH]_0/[Hex\text{-}NH_2]_0$ ratios. For all polymerizations, $[M]_0 = 0.2$ M, $[DMAP]_0/[I]_0 = 1$, $[M]_0/[AcOH]_0 = 1$. $[M]_0/[I]_0 = 50$ except for (d), (f) and (g).

conversion in the presence of Hex-NH_2, but <20% consumption of Trp-NCA through AMM. In contrast, triethylamine (TEA) with a slightly higher basicity (pK_{BH^+} = 18.8) mediated AMM polymerization in which ∼55% monomer was polymerized under identical conditions. Therefore, the fine-tuning of basicity of catalytic bases was crucial to mediate NAM polymerization in an accelerated manner.

Improved Control over Molecular Weights in the Presence of Organic Acids

Encouraged by the accelerated polymerization of Trp-NCA by DMAP, we continued to check the control over MWs of resulting PLWs. Unfortunately, the obtained MWs were much larger than theoretical values calculated from feeding $[M]_0/[I]_0$, even though GPC suggested monomodal peaks for all polymerizations with acceptable dispersity ($Đ = M_w/M_n$ < 1.25) (Figure S9). Specifically, the M_n at $[M]_0/[I]_0$ = 50, 100, and 200 was determined to be 19.9, 27.2, and 41.9 kDa, which was 2.1, 1.4, and 1.1 times higher than the theoretical M_n (Table S3). The $[M]_0/[I]_0$-dependent MW control resembled that of CE-catalyzed cooperative covalent polymerization (CCP) system,[43] suggesting that the discrepancy between obtained and theoretical MWs stemmed from the two-stage kinetics with a slower first stage. The growing PLW chains in the second stage outpaced those in the first stage, yielding high-MW polypeptides and short oligomers (Figure S10). The increase in $[M]_0/[I]_0$ thus allowed for the shorter chains to catch up with the longer chains, leading to better MW control. Indeed, the *in situ* FTIR analysis revealed an obvious coil-to-helix transition during DMAP-catalyzed polymerization of Trp-NCA, which was the structural origin of the two-stage kinetics (Figure S11). Moreover, the polymerization of the racemic DL-tryptophan NCA monomer, with one-stage kinetics due to the lack of conformational transition, generated a polypeptide with a predictable MW (Figure S11 and Table S3), further confirming that the poor MW control was correlated to the two-stage kinetics ($k_1 = 0.36\ h^{-1}$, $k_2 = 1.55\ h^{-1}$). In fact, the introduction of the base played an insignificant role in MW control, as the slow polymerization under anhydrous conditions in the absence of DMAP yielded PLWs with similar MWs as those in the presence of DMAP (*vide infra*).

With sufficient understanding of the MW control of DMAP-catalyzed polymerization of Trp-NCA, we incorporated acetic acid (AcOH) into the polymerization solution to alter the kinetic profile (Figure 2a). The first-order, one-stage kinetics ($k_{obs} = 1.09\ h^{-1}$) was confirmed by *in situ* NMR characterization (Figures 2b and S12), which was consistent with previous reports.[53] Further investigation revealed that an equimolar amount of AcOH relative to the monomer was necessary to generate polypeptides with predictable MWs (Figure S13 and Table S4), in good agreement with recent reports.[45,47,48,53] In addition, using an equimolar amount of DMAP relative to the initiator resulted in a narrower molecular weight distribution (Figure S13 and Table S5), presumably by suppressing AMM side reactions.[51] On this basis, the optimal feed ratio was determined to be $[M]_0$:$[AcOH]_0$:$[DMAP]_0$:$[I]_0$ = 50:50:1:1, which enabled accelerated polymerization and afforded polypeptides with predictable molecular weights and narrow dispersity. As a result, the addition of AcOH significantly reduced the MWs of the resulting PLW at $[M]_0/[I]_0$ = 50 ($[M]_0/[AcOH]_0 = 1$) from 19.9 to 10.6 kDa (Figure 2c), which was consistent with the designed value (i.e., 9.4 kDa). PLWs with various MWs ranging from 10.6 to 36.6 kDa were thus

https://doi.org/10.1021/acs.macromol.6c00471
Macromolecules 2026, 59, 6854−6863

prepared in an efficient manner through the change in feeding $[M]_0/[I]_0$ (Figure 2d, Table 1, and Figure S14). In fact, the one-stage kinetics allowed for the preparation of oligo(L-tryptophan) at the design degree of polymerization (DP) = 10 and 20 (Figure S15 and Table S6), where conventional CCP exhibited poor MW control with the two-stage kinetics.[58] In addition, the linear relationship between MWs and monomer conversion indicates a living polymerization process (Figure 2e, Figure S16, and Table S7). The living polymerization behavior facilitated by AcOH/DMAP allowed for the efficient chain extension to prepare block copolypeptides, with a clear MW shift on GPC traces (Figure S17). MALDI-TOF MS results also suggested expected end-groups from Hex-NH_2 initiation with negligible chain terminations (Figures 2f and S18).

Table 1. Polymerization of Trp-NCA in the Presence of AcOH/DMAP[a]

entry	$[M]_0/[I]_0$	t^b (h)	$M_{n,theo.}$ (kDa)	$M_{n,NMR}{}^c$ (kDa)	$M_{n,GPC}{}^d$ (kDa)	$Đ^d$
1[e]	50	48	9.4		20.0	1.19
2[f]	50	3	9.4		19.9	1.19
3	50	3	9.4	9.6	10.6	1.05
4	75	4	14.1	14.3	16.1	1.08
5	100	4	18.7	19.3	19.8	1.05
6	150	6	28.0	27.7	29.7	1.05
7	200	8	37.3	36.9	36.6	1.05
8[g]	50 + 50	3 + 3	9.4/18.7		10.5/18.5	1.05

[a]All polymerizations were conducted at room temperature in DCM/DMF (1:1, v/v) cosolvents with *n*-hexylamine as the initiator and AcOH/DMAP as the catalysts. $[M]_0$ = 0.2 M, $[DMAP]_0/[I]_0$= 1, $[M]_0/[AcOH]_0$ = 1. [b]The polymerization time reached 95% monomer conversion. [c]Determined by NMR. [d]Determined by GPC; d*n*/d*c* = 0.125. [e]Polymerization was carried out in the absence of AcOH or DMAP. [f]Polymerization was carried out in the absence of AcOH. [g]Preparation of diblock copolypeptides was achieved through sequential addition of Trp-NCA monomers.

AcOH/DMAP mixtures, where equimolar of DMAP and Hex-NH_2 was mixed with an increasing amount of AcOH, aiming to check the protonation of two organic bases under polymerization conditions. As the $[AcOH]_0/[Hex\text{-}NH_2]_0$ ratio increased, obvious downfield shifts were observed for both the methine protons adjacent to pyridine N and the methyl protons next to the tertiary amine in DMAP, suggesting the protonation of DMAP (Figure S19). Meanwhile, the protonation of Hex-NH_2 was validated from the downfield shift of α-protons of Hex-NH_2 (Figure S19). Nevertheless, the relatively weak acidity of AcOH guaranteed partial protonation of two organic bases even though the organic acids were in excess. For instance, roughly 22% of the pyridine N, 40% of the tertiary amine, and 47% of the primary amine remained nonprotonated at $[AcOH]_0/[Hex\text{-}NH_2]_0$ = 50 (Figure 2g). The small fraction of nonprotonated DMAP, while unlikely to deprotonate NCA to initiate the polymerization

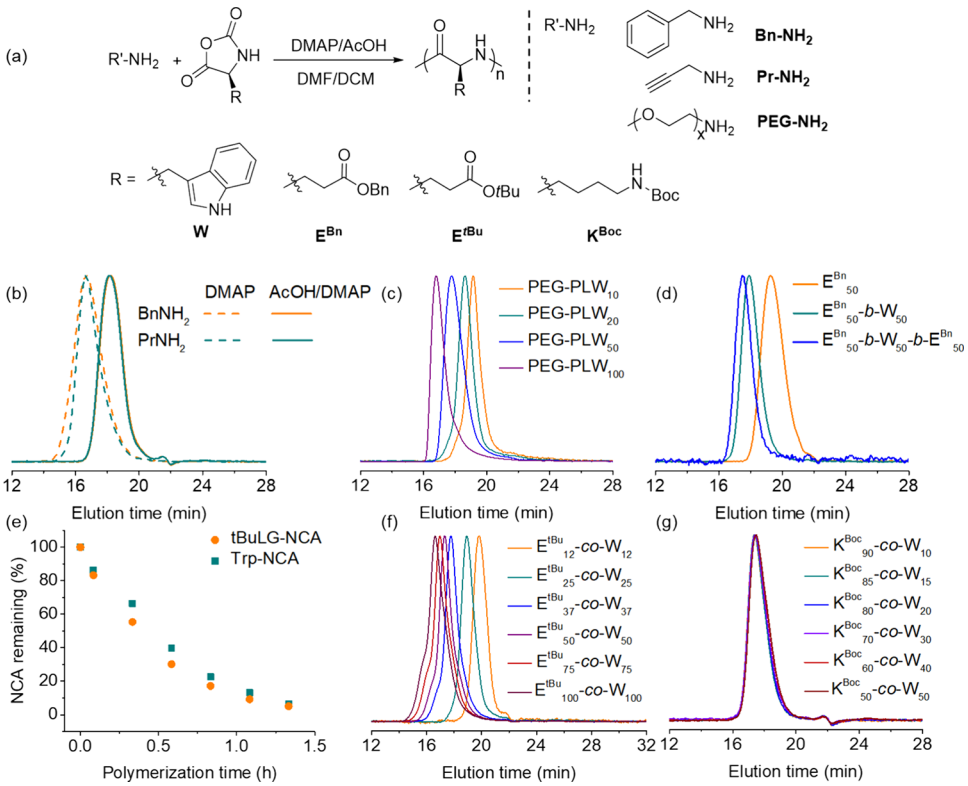

Figure 3. AcOH/DMAP-mediated preparation of tryptophan-containing polypeptide materials. (a) Chemical structures of various primary amine initiators and NCA monomers used in this study. (b) Normalized GPC-LS traces of polypeptides with different amine initiators in the presence and absence of AcOH. $[M]_0/[I]_0$ = 50. (c) Normalized GPC-LS traces of PEG-*b*-PLW initiated with PEG_{2k}-NH_2 at various $[M]_0/[I]_0$ ratios. (d) Normalized GPC-LS traces of triblock copolypeptides E^{Bn}-*b*-W-*b*-E^{Bn} and its synthetic intermediates. (e) Semilogarithmic kinetic plot of copolymerization of tBuLG-NCA and Trp-NCA in the presence AcOH/DMAP. (f, g) Normalized GPC-LS traces of the resulting statistical copolypeptides E^{tBu}-*co*-W (f) and K^{Boc}-*co*-W (g) at various monomer ratios. For all polymerizations, $[M]_0$ = 0.2 M, $[DMAP]_0/[I]_0$ = 1, $[M]_0/[AcOH]_0$ = 1.

https://doi.org/10.1021/acs.macromol.6c00471
Macromolecules 2026, 59, 6854−6863

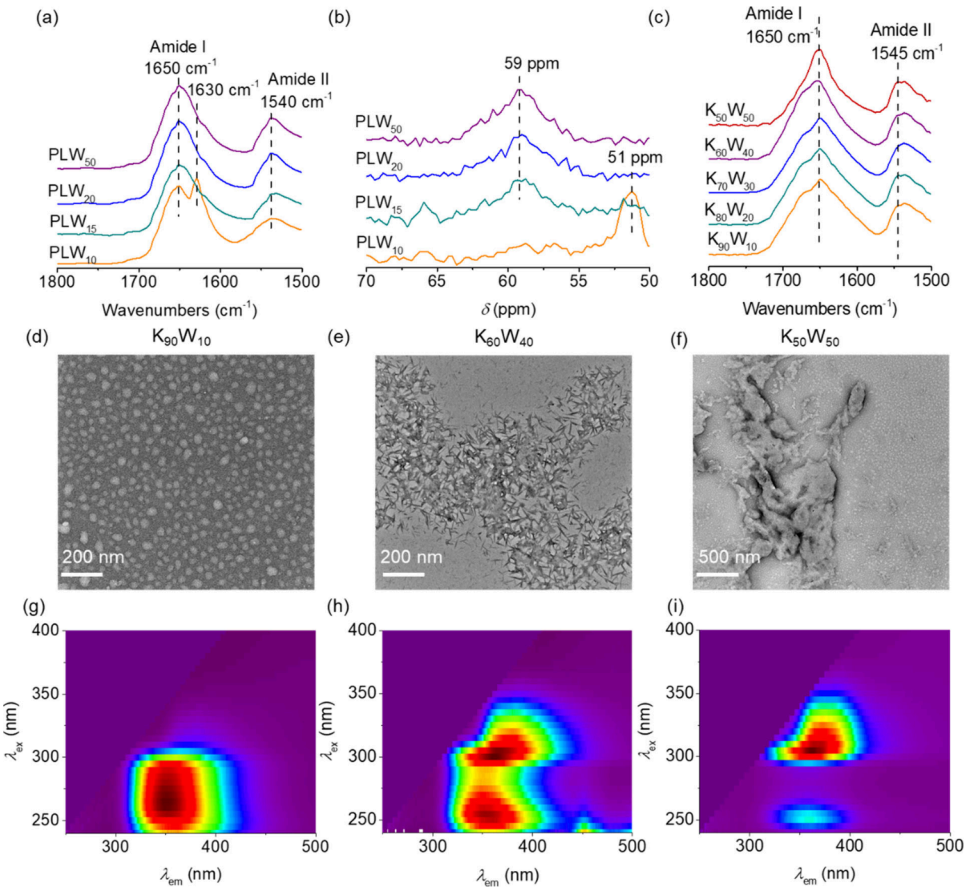

Figure 4. The impact of tryptophan content on secondary structure, self-assembly behavior, and fluorescent properties of PLW-based materials. (a) FTIR spectra showing the secondary structure of PLW in solid phase with different DP. (b) Expanded ^{13}C CP/MAS NMR spectra of the α-carbon region for PLW with different DP. (c) FTIR spectra showing the secondary structure of KW statistical copolypeptides in solid phase with different DP. (d–f) HRTEM images of the W content-dependent morphology of K_x-*co*-W_y nanoassemblies. (g–i) The 3D fluorescence spectra of the differential polarity and water interactions of tryptophan residues of copolypeptides in ddH_2O. c = 0.5 mg/mL.

through AMM mechanism in the presence of excessive AcOH, might activate the monomers for accelerated polymerization. In contrast, stronger acids like HCl and trifluoroacetic acid (TFA) would completely protonate the amino groups and block the polymerization, with negligible monomer conversion after 48 h (Figures S19 and S20).

Preparation of Various Polypeptide Materials Based on PLW

The AcOH/DMAP strategy could be further extended to other initiators or monomers (Figure 3a). For instance, 3-aminopropyne and benzylamine were used to initiate the polymerization of Trp-NCA ($[M]_0/[I]_0$ = 50), which completed within 3 h, producing PLWs with predictable MWs and narrow dispersity ($Đ$ < 1.20) (Figure 3b and Table S8). Meanwhile, AcOH/DMAP was further introduced into the polymerization initiated by PEGylated amines (M_n = 2.0 kDa). By modulating the $[M]_0/[I]_0$ ratio, various PEG-*b*-PLW with monomodal peaks were successfully obtained (Figure 3c and Table S9).

Moreover, the living nature of AcOH/DMAP-mediated polymerization enabled efficient chain extensions. Triblock copolypeptides with ABA sequence were synthesized within 5 h with negligible side reactions through sequential addition of BLG-NCA and Trp-NCA in the presence of AcOH/DMAP (Figure 3d and Table S10). The obtained MWs agree well with the expected MWs, with low dispersity ($Đ$ < 1.10) observed for all intermediates and final triblock copolypeptides. The clear MW shift on GPC traces substantiated the high end-group fidelity for chain extension.

To prepare water-soluble polypeptides with tryptophan residues, Trp-NCA was copolymerized with NCA monomers bearing protected side chains. Because the side-chain indole ring is sensitive to several standard deprotection reagents (i.e., oxidation and other side reactions),[59] NCAs bearing acid-labile side chains were used, including γ-*tert*-butyl-$_L$-glutamate NCA (tBuLG-NCA) with *tert*-butyl (tBu) protecting groups and N^{ε}-*tert*-butoxycarbonyl-$_L$-lysine NCA (BLL-NCA) bearing *tert*-butoxycarbonyl (Boc) moieties. Following AcOH/DMAP-mediated copolymerization with Trp-NCA, the resulting copolypeptides were treated with TFA to remove the protecting groups, affording water-soluble copolypeptides (Scheme S1). Surprisingly, *in situ* NMR kinetic analysis indicated that the consumption rate of Trp-NCA was comparable with that of tBuLG-NCA and BLL-NCA (Figure 3e and Figures S21 and S22), even though the polymerization rate was distinctly different in the absence of AcOH/DMAP. By varying the ratio between two monomers, several copolypeptides were prepared with predictable MWs and narrow dispersity (Figure 3f,g, Figure S23, and Tables S11 and S12). The copolymerization thus allows for the access to a series of water-soluble, cationic or anionic, tryptophan-containing copolypeptides with statistical sequences, which would be difficult to prepare in the absence of AcOH/DMAP.[28]

https://doi.org/10.1021/acs.macromol.6c00471
Macromolecules 2026, 59, 6854–6863

Composition-Dependent Assembly Behaviors and Fluorescent Properties

Tryptophan residues play a pivotal role in proteins, where their bulky aromatic indole side chains contribute to the stabilization of folded structures (e.g., tryptophan cages and WW domains) or participate in key recognition events. Notably, the tryptophan side chains often reside at hydrophobic or interfacial regions in globular proteins, whose fluorescent emission responds strongly to changes in local polarity, packing, and conformational dynamics.[60,61] Motivated by these features, we designed a series of poly(L-lysine)-*co*-poly(L-tryptophan) random copolypeptides by deprotecting K^{Boc}-*co*-W with various compositions. The copolypeptides were termed K_xW_y, which were used to probe the impact of tryptophan content on the self-assembly behaviors and fluorescent properties.

The secondary structure of the copolypeptides was first studied, which is critical to determine their assembly behaviors. Homopolypeptide PLW exhibited length-dependent secondary structures, with characteristic Amide I peak (i.e., 1650 cm^{-1}) that corresponded to α-helical structure when the degree of polymerization (DP) was greater than 10 (Figure 4a). At DP = 10, PLW adopted both α-helical and β-sheet conformations, as evidenced by the FTIR characterization with two Amide I peaks (the latter one at 1630 cm^{-1}). Meanwhile, solid state ^{13}C cross-polarization (CP) magic angle spinning (MAS) NMR of PLW confirmed the DP-dependent conformation in solid state, where the chemical shift of backbone Cα carbon of α-helical PLW_{15} and β-sheet PLW_{10} was observed at 59 and 51 ppm, respectively (Figure 4b). Similarly, the backbone carbonyl also exhibited a shift from 172 to 176 ppm when the DP increased from 10 to 15 (Figure S24). Additionally, poly(D-tryptophan) (PDW) and poly(DL-tryptophan) (PDLW) were prepared from corresponding monomers with different chirality. While the polymerization rate of D-monomer (k_{obs} = 1.22 h^{-1}) resembled that of L-monomer, the polymerization of DL monomer proceeded in a slower rate (k_{obs} = 0.56 h^{-1}), which was attributed to the absence of helix-induced acceleration.[47] Nevertheless, the catalytic system afforded good MW control for both PDW and PDLW with predictable MWs and narrow dispersity (Figure S25 and Table S13). Circular dichroism (CD) confirmed the chirality differences of the polypeptide materials. Specifically, CD spectra of PLW revealed the characteristic α-helical signature with a band near 220 nm, albeit with the interference of absorption from side-chain indole groups. Incorporation of the tryptophan−tryptophan motif into the polypeptide backbone induces a sign inversion of the characteristic CD feature (~230 nm) (Figure S25), consistent with backbone-imposed changes in indole−indole geometry and the associated exciton coupling.[62] Meanwhile, the D-enantiomers exhibit equal-magnitude but opposite-sign spectral features under identical conditions.[63] Additionally, FTIR analysis suggested the α-helical conformations for all copolypeptides in solid states, with obvious Amide I (1650 cm^{-1}) and Amide II bands (1545 cm^{-1}) (Figure 4c).

The copolypeptides were dissolved in water, which spontaneously formed nanoparticles. High-resolution transmission electron microscopy (HRTEM) analysis revealed that $K_{90}W_{10}$ with low tryptophan content mainly assembled into uniform, spherical nanoparticles (Figure 4d). As the tryptophan content increased, the assemblies progressively evolved from spherical nanoparticles to fiber-like morphologies for $K_{60}W_{40}$ (Figure 4e). When tryptophan residue content reached 50 mol %, large aggregates were observed. (Figure 4f). The hydrophobic interactions and $\pi-\pi$ stacking between tryptophan side chains likely drove the assembly of the copolypeptides.[64] Meanwhile, the cation−π interactions between cationic lysine and tryptophan side chains may also have an impact on the morphology, which was confirmed by nuclear Overhauser effect (NOE) NMR studies (Figure S26). The KW series of polypeptides thus served as a good model for the assembly studies based on cation−π interactions.[65] Preliminary studies suggested that both pH and salt conditions introduced additional complexity into the self-assembly process (Figure S27).

The different assembly behaviors of copolypeptides were further probed by three-dimensional fluorescence spectroscopy, which provided a comprehensive insight into the fluorescent characteristics by simultaneously acquiring the excitation−emission matrix (EEM) data.[66,67] The spectra of $K_{90}W_{10}$ exhibited a well-defined excitation−emission peak with λ_{ex} = 265 nm and λ_{em} = 350 nm (Figure 4g). Considering the low percentage of tryptophan residues, the peak likely originated from the monomeric indole side chains in a hydrophobic environment. The increase in tryptophan content not only increased the density of indole groups, but also directed the ordered stacking of fluorophores as evidenced by the fibril morphologies. As a result, a new excitation−emission peak appeared with λ_{ex} = 305 nm and λ_{em} = 360 nm for $K_{60}W_{40}$ (Figure 4h), which was attributed to the exciton coupling that lowered the excitation energy. Interestingly, further increase in tryptophan content led to the disappearance of the monomeric excitation−emission peak for $K_{50}W_{50}$ (Figure 4i), suggesting the strong interactions between excitons in the ordered assemblies. The tryptophan residues thus served as sensitive probes to characterize the structure and assembly behavior of copolypeptides, whose fluorescent properties were highly dependent on the local environment of the fluorophores.

CONCLUSION

In conclusion, we developed a robust and general strategy for the controlled synthesis of PLW and its copolypeptide analogue via NCA ROP. Using AcOH/DMAP as kinetic modulators significantly improves polymerization rate and MW control, yielding Trp-based polypeptides with predictable MWs, low dispersity, and well-defined structures. The bicyclic, π-conjugated indole side chains mediated interesting assembly behaviors and fluorescent properties. We therefore offered a facile strategy to prepare various tryptophan-containing materials, boosting the downstream property studies and applications of the materials.

ASSOCIATED CONTENT

Data Availability Statement

Deposition number 2523143 contains the supplementary crystallographic data for this paper.

Supporting Information

The Supporting Information is available free of charge at https://pubs.acs.org/doi/10.1021/acs.macromol.6c00471.

Materials, instrumentations, experimental section and the characterizations of monomers, random copolymers and multiblock copolymers (^1H NMR,^{13}C NMR, kinetic study, FT-IR spectra, ^{13}C CP MAS NMR, MALDI-TOF, GPC characterization results, NMR titration, single crystals, NOESY) (PDF)

https://doi.org/10.1021/acs.macromol.6c00471
Macromolecules 2026, 59, 6854−6863

AUTHOR INFORMATION

Corresponding Authors

Jianjun Cheng − *Department of Materials Science and Engineering and Research Center for Industries of the Future, Westlake University, Hangzhou, Zhejiang 310030, China; Institute of Advanced Technology, Westlake Institute for Advanced Study, Hangzhou, Zhejiang 310024, China;* orcid.org/0000-0003-2561-9291; Email: chengjianjun@westlake.edu.cn

Ziyuan Song − *Institute of Functional Nano & Soft Materials (FUNSOM), Jiangsu Key Laboratory for Carbon-Based Functional Materials and Devices, Soochow University, Suzhou, Jiangsu 215123, China;* orcid.org/0000-0002-3165-3712; Email: zysong@suda.edu.cn

Chengjie Sun − *Department of Materials Science and Engineering, Westlake University, Hangzhou, Zhejiang 310030, China; Institute of Advanced Technology, Westlake Institute for Advanced Study, Hangzhou, Zhejiang 310024, China;* orcid.org/0000-0001-6038-1616; Email: sunchengjie@westlake.edu.cn

Authors

Chenlin Ji − *School of Materials Science and Engineering, Zhejiang University, Hangzhou, Zhejiang 310058, China; Department of Materials Science and Engineering, Westlake University, Hangzhou, Zhejiang 310030, China*

Tingting Cao − *Department of Materials Science and Engineering, Westlake University, Hangzhou, Zhejiang 310030, China*

Luyao Wang − *Department of Materials Science and Engineering, Westlake University, Hangzhou, Zhejiang 310030, China; Institute of Advanced Technology, Westlake Institute for Advanced Study, Hangzhou, Zhejiang 310024, China*

Zhuohang Zhou − *Department of Materials Science and Engineering, Westlake University, Hangzhou, Zhejiang 310030, China; Institute of Advanced Technology, Westlake Institute for Advanced Study, Hangzhou, Zhejiang 310024, China*

Yu Zhao − *Department of Materials Science and Engineering, Westlake University, Hangzhou, Zhejiang 310030, China; Institute of Advanced Technology, Westlake Institute for Advanced Study, Hangzhou, Zhejiang 310024, China*

Xingliang Liu − *Department of Materials Science and Engineering, Westlake University, Hangzhou, Zhejiang 310030, China; Institute of Advanced Technology, Westlake Institute for Advanced Study, Hangzhou, Zhejiang 310024, China; Department of Biomedical Engineering, School of Engineering, China Pharmaceutical University, Nanjing, Jiangsu 211198, China;* orcid.org/0009-0008-5431-1185

Complete contact information is available at: https://pubs.acs.org/10.1021/acs.macromol.6c00471

Author Contributions

C.J. conceived the concept, designed this research and drafted the manuscript. C.J., T.C., L.W., Z.Z., Y.Z., and X.L. performed experiments and analyzed the data. C.S., Z.S., and J.C. supervised this research and revised the manuscript. All authors approved the final version of the manuscript.

Funding

"Pioneer" and "Leading Goose" R&D Program of Zhejiang (2024SDXHDX0004). National Natural Science Foundation of China (52233015 for J.C. and 22101194 for Z.S.). New Cornerstone Investigator Program, New Cornerstone Science Foundation. Zhejiang Province Postdoctoral Research Project Selective Support (ZJ2025026, L.W.).

Notes

The authors declare no competing financial interest.

ACKNOWLEDGMENTS

This work was supported by "Pioneer" and "Leading Goose" R&D Program of Zhejiang (2024SDXHDX0004), National Natural Science Foundation of China (52233015 for J. Cheng and 22101194 for Z. Song) and Zhejiang Province Postdoctoral Research Project Selective Support (ZJ2025026, L.W). We acknowledge the support of the New Cornerstone Investigator Program, New Cornerstone Science Foundation. We thank Dr. Yinjuan Chen, Dr. Xingyu Lu, Dr. Xiaohe Miao, Dr. Zhong Chen, Dr. Xiaohuo Shi, Ms. Danyu Gu, Ms. Xin Li and Ms. Yuqian Sun from Instrumentation and Service Center for Molecular Sciences (ISCMS) at Westlake University for the assistance in measurement and data interpretation.

REFERENCES

(1) Khemaissa, S.; Sagan, S.; Walrant, A. Tryptophan, an amino-acid endowed with unique properties and its many roles in membrane proteins. *Crystals.* **2021**, *11* (9), 1032−1045.

(2) Shao, J.; Kuiper, B. P.; Thunnissen, A. W. H.; Cool, R. H.; Zhou, L.; Huang, C.; Dijkstra, B. W.; Broos, J. The role of tryptophan in π interactions in proteins: an experimental approach. *J. Am. Chem. Soc.* **2022**, *144* (30), 13815−13822.

(3) Situ, A. J.; Kang, S. M.; Frey, B. B.; An, W.; Kim, C.; Ulmer, T. S. Membrane anchoring of α-helical proteins: role of tryptophan. *J. Phys. Chem. B* **2018**, *122* (3), 1185−1194.

(4) Barik, S. The uniqueness of tryptophan in biology: properties, metabolism, interactions and localization in proteins. *Int. J. Mol. Sci.* **2020**, *21* (22), 8776−8798.

(5) Xue, C.; Li, G.; Zheng, Q.; Gu, X.; Shi, Q.; Su, Y.; Chu, Q.; Yuan, X.; Bao, Z.; Lu, J.; Li, L. Tryptophan metabolism in health and disease. *Cell Metab.* **2023**, *35* (8), 1304−1326.

(6) Nguyen, A. K.; Molley, T. G.; Kardia, E.; Ganda, S.; Chakraborty, S.; Wong, S. L.; Ruan, J.; Yee, B. E.; Mata, J.; Vijayan, A.; Kumar, N.; Tilley, R. D.; Waters, S. A.; Kilian, K. A. Hierarchical assembly of tryptophan zipper peptides into stress-relaxing bioactive hydrogels. *Nat. Commun.* **2023**, *14* (1), 6604−6617.

(7) Takekiyo, T.; Wu, L.; Yoshimura, Y.; Shimizu, A.; Keiderling, T. A. Relationship between hydrophobic interactions and secondary structure stability for Trpzip β-hairpin peptides. *Biochemistry.* **2009**, *48* (7), 1543−1552.

(8) Hanay, S. B.; Brougham, D. F.; Dias, A. A.; Heise, A. Investigation of the triazolinedione (TAD) reaction with tryptophan as a direct route to copolypeptide conjugation and cross-linking. *Polym. Chem.* **2017**, *8* (43), 6594−6597.

(9) Kimmins, S. D.; Hanay, S. B.; Murphy, R.; O'Dwyer, J.; Ramalho, J.; Ryan, E. J.; Kearney, C. J.; O'Brien, F. J.; Cryan, S. A.; Fitzgerald-Hughes, D.; Heise, A. Antimicrobial and degradable triazolinedione (TAD) crosslinked polypeptide hydrogels. *J. Mater. Chem. B* **2021**, *9* (27), 5456−5464.

(10) Hanay, S. B.; O'Dwyer, J.; Kimmins, S. D.; de Oliveira, F. C. S.; Haugh, M. G.; O'Brien, F. J.; Cryan, S. A.; Heise, A. Facile approach to covalent copolypeptide hydrogels and hybrid organohydrogels. *ACS Macro Lett.* **2018**, *7* (8), 944−949.

(11) Bielas, R.; Fattah, S.; Mielańczyk, Ł.; Pozdeev, G.; Cryan, S. A.; Heise, A. Compositional influence of cross-linked polyion hydrogels from poly(L-lysine) and poly(L-glutamic acid) on their properties for

potential skin applications. *Macromol. Chem. Phys.* **2024**, *225* (20), No. 2400201.
(12) Fan, Z.; Sun, L.; Huang, Y.; Wang, Y.; Zhang, M. Bioinspired fluorescent dipeptide nanoparticles for targeted cancer cell imaging and real-time monitoring of drug release. *Nat. Nanotechnol.* **2016**, *11* (4), 388−394.
(13) Yang, Y.; Chen, L.; Sun, M.; Wang, C.; Fan, Z.; Du, J. Biodegradable polypeptide-based vesicles with intrinsic blue fluorescence for antibacterial visualization. *Chin. J. Polym. Sci.* **2021**, *39* (11), 1412−1420.
(14) Shih, C.; Museth, A. K.; Abrahamsson, M.; Blanco-Rodriguez, A. M.; Di Bilio, A. J.; Sudhamsu, J.; Crane, B. R.; Ronayne, K. L.; Towrie, M.; Vlcek, A., Jr.; Richards, J. H.; Winkler, J. R.; Gray, H. B. Tryptophan-accelerated electron flow through proteins. *Science.* **2008**, *320* (5884), 1760−1762.
(15) Salzmann, C. G.; Lee, G. K. C.; Ward, M. A. H.; Chu, B. T. T.; Green, M. L. H. Highly hydrophilic and stable polypeptide/single-wall carbon nanotube conjugates. *J. Mater. Chem.* **2008**, *18* (17), 1977−1983.
(16) Guo, Y.; Kalathur, R. C.; Liu, Q.; Kloss, B.; Bruni, R.; Ginter, C.; Kloppmann, E.; Rost, B.; Hendrickson, W. A. Protein structure. Structure and activity of tryptophan-rich TSPO proteins. *Science.* **2015**, *347* (6221), 551−555.
(17) Yeh, P. S.; Li, C. C.; Lu, Y. S.; Chiang, Y. W. Structural Insights into the Binding and Degradation Mechanisms of Protoporphyrin IX by the Translocator Protein TSPO. *JACS. Au.* **2023**, *3* (10), 2918−2929.
(18) Deming, T. J. *Polypeptide and Polypeptide Hybrid Copolymer Synthesis via NCA Polymerization*; Springer, 2006; Vol. *202*, pp 1−18.
(19) Wu, Y.; Chen, K.; Wang, J.; Chen, M.; Dai, W.; Liu, R. Recent advances and future developments in the preparation of polypeptides via *N*-carboxyanhydride (NCA) ring-opening polymerization. *J. Am. Chem. Soc.* **2024**, *146* (35), 24189−24208.
(20) Deming, T. J. Synthesis of side-chain modified polypeptides. *Chem. Rev.* **2016**, *116* (3), 786−808.
(21) Rasines Mazo, A.; Allison-Logan, S.; Karimi, F.; Chan, N. J.; Qiu, W.; Duan, W.; O'Brien-Simpson, N. M.; Qiao, G. G. Ring opening polymerization of α-amino acids: advances in synthesis, architecture and applications of polypeptides and their hybrids. *Chem. Soc. Rev.* **2020**, *49* (14), 4737−4834.
(22) Song, Z.; Fu, H.; Wang, R.; Pacheco, L. A.; Wang, X.; Lin, Y.; Cheng, J. Secondary structures in synthetic polypeptides from *N*-carboxyanhydrides: design, modulation, association, and material applications. *Chem. Soc. Rev.* **2018**, *47* (19), 7401−7425.
(23) Yamada, S.; Atsushi, S.; Goto, M.; Endo, T. Facile synthesis of poly(L-tryptophan) through polycondensation of activated urethane derivatives. *J. Polym. Sci. A Polym. Chem.* **2013**, *51* (21), 4565−4571.
(24) Li, L.; Cen, J.; Li, W.; Pan, W.; Zhang, Y.; Yin, H.; Hu, J.; Liu, S. A general strategy toward synthesis of well-defined polypeptides with complex chain topologies. *CCS Chem.* **2022**, *4* (12), 3864−3877.
(25) Fu, X.; Lin, X.; Wang, M.; Ding, Z.; Ma, G.; Wang, B.; Li, Y. One-step synthesis of sequence-defined polypeptide-*block*-polyester by Lewis pair-catalyzed chemo-selective copolymerization. *Macromolecules.* **2024**, *57* (12), 5691−5701.
(26) Xiang, Y.; Si, J.; Zhang, Q.; Liu, Y.; Guo, H. Homogeneous graft copolymerization and characterization of novel artificial glycoprotein: Chitosan-poly(L-tryptophan) copolymers with secondary structural side chains. *J. Polym. Sci. A Polym. Chem.* **2009**, *47* (3), 925−934.
(27) Santiveri, C. M.; Jiménez, M. A. *Tryptophan residues: Scarce in proteins but strong stabilizers of β-hairpin peptides.* **2010**, *94* (6), 779−790.
(28) Eom, K. H.; Baek, S.; Kim, I. *N*-Heterocyclic carbene-catalyzed random copolymerization of *N*-carboxyanhydrides of α-amino acids. *Polymers.* **2021**, *13* (21), 3674−3684.
(29) Baumgartner, R.; Fu, H.; Song, Z.; Lin, Y.; Cheng, J. Cooperative polymerization of α-helices induced by macromolecular architecture. *Nat. Chem.* **2017**, *9* (7), 614−622.
(30) Song, Z.; Fu, H.; Baumgartner, R.; Zhu, L.; Shih, K.-C.; Xia, Y.; Zheng, X.; Yin, L.; Chipot, C.; Lin, Y.; Cheng, J. Enzyme-mimetic self-catalyzed polymerization of polypeptide helices. *Nat. Commun.* **2019**, *10* (1), 5470−5477.
(31) Yuan, J.; Zhang, Y.; Li, Z.; Wang, Y.; Lu, H. A S-Sn Lewis pair-mediated ring-opening polymerization of α-amino acid *N*-carboxyanhydrides: Fast kinetics, high molecular weight, and facile bioconjugation. *ACS Macro Lett.* **2018**, *7* (8), 892−897.
(32) Wu, Y.; Zhang, D.; Ma, P.; Zhou, R.; Hua, L.; Liu, R. Lithium hexamethyldisilazide initiated superfast ring opening polymerization of α-amino acid *N*-carboxyanhydrides. *Nat. Commun.* **2018**, *9* (1), 5297−5307.
(33) Chen, C.; Fu, H.; Baumgartner, R.; Song, Z.; Lin, Y.; Cheng, J. Proximity-induced cooperative polymerization in "hinged" helical polypeptides. *J. Am. Chem. Soc.* **2019**, *141* (22), 8680−8683.
(34) Jacobs, J.; Pavlović, D.; Prydderch, H.; Moradi, M.-A.; Ibarboure, E.; Heuts, J. P. A.; Lecommandoux, S.; Heise, A. Polypeptide nanoparticles obtained from emulsion polymerization of amino acid *N*-carboxyanhydrides. *J. Am. Chem. Soc.* **2019**, *141* (32), 12522−12526.
(35) Zhao, W.; Lv, Y.; Li, J.; Feng, Z.; Ni, Y.; Hadjichristidis, N. Fast and selective organocatalytic ring-opening polymerization by fluorinated alcohol without a cocatalyst. *Nat. Commun.* **2019**, *10* (1), 3590.
(36) Lv, W.; Wang, Y.; Li, M.; Wang, X.; Tao, Y. Precision synthesis of polypeptides via living anionic ring-opening polymerization of *N*-carboxyanhydrides by tri-thiourea catalysts. *J. Am. Chem. Soc.* **2022**, *144* (51), 23622−23632.
(37) Wang, X.; Song, Z.; Tan, Z.; Zhu, L.; Xue, T.; Lv, S.; Fu, Z.; Zheng, X.; Ren, J.; Cheng, J. Facile synthesis of helical multiblock copolypeptides: minimal side reactions with accelerated polymerization of *N*-carboxyanhydrides. *ACS Macro Lett.* **2019**, *8* (11), 1517−1521.
(38) Song, Z.; Fu, H.; Wang, J.; Hui, J.; Xue, T.; Pacheco, L. A.; Yan, H.; Baumgartner, R.; Wang, Z.; Xia, Y.; Wang, X.; Yin, L.; Chen, C.; Rodríguez-López, J.; Ferguson, A. L.; Lin, Y.; Cheng, J. Synthesis of polypeptides via bioinspired polymerization of *in situ* purified *N*-carboxyanhydrides. *Proc. Natl. Acad. Sci. U. S. A.* **2019**, *116* (22), 10658−10663.
(39) Li, Q.; Lan, Y.; Wang, W.; Ji, G.; Li, X.; Song, Z. Polymerization of *N*-carboxyanhydride in cosolvents: the balance between the polymerization rate and molecular weight control. *Macromolecules.* **2023**, *56* (17), 7023−7031.
(40) Uchida, C.; Iizuka, Y.; Ohta, E.; Wakamatsu, K.; Oya, M. Synthesis and properties of high-molecular-weight polypeptides containing tryptophan ii. copolypeptides of tryptophan with various amino acids. *Bull. Chem. Soc. Jpn.* **1996**, *69* (3), 791−796.
(41) Jadrich, C. N.; Pane, V. E.; Lin, B.; Jones, G. O.; Hedrick, J. L.; Park, N. H.; Waymouth, R. M. A cation-dependent dual activation motif for anionic ring-opening polymerization of cyclic esters. *J. Am. Chem. Soc.* **2022**, *144* (19), 8439−8443.
(42) Khemaissa, S.; Walrant, A.; Sagan, S. Tryptophan, more than just an interfacial amino acid in the membrane activity of cationic cell-penetrating and antimicrobial peptides. *Q. Rev. Biophys.* **2022**, *55*, e10.
(43) Xia, Y.; Song, Z.; Tan, Z.; Xue, T.; Wei, S.; Zhu, L.; Yang, Y.; Fu, H.; Jiang, Y.; Lin, Y.; Lu, Y.; Ferguson, A. L.; Cheng, J. Accelerated polymerization of *N*-carboxyanhydrides catalyzed by crown ether. *Nat. Commun.* **2021**, *12* (1), 732−740.
(44) Siefker, D.; Williams, A. Z.; Stanley, G. G.; Zhang, D. Organic acid promoted controlled ring-opening polymerization of α-amino acid-derived *N*-thiocarboxyanhydrides (NTAs) toward well-defined polypeptides. *ACS Macro Lett.* **2018**, *7* (10), 1272−1277.
(45) Liu, X.; Huang, J.; Wang, J.; Sheng, H.; Yuan, Z.; Wang, W.; Li, W.; Song, Z.; Cheng, J. Accelerated and controlled polymerization of *N*-carboxyanhydrides assisted by acids. *CCS Chem.* **2025**, *7* (9), 2769−2780.
(46) Wang, S.; Lu, M. Y.; Wan, S. K.; Lyu, C. Y.; Tian, Z. Y.; Liu, K.; Lu, H. Precision synthesis of polysarcosine *via* controlled ring-opening polymerization of *N*-carboxyanhydride: fast kinetics, ultrahigh molecular weight, and mechanistic insights. *J. Am. Chem. Soc.* **2024**, *146* (8), 5678−5692.
(47) Liu, W.; Deng, X.; Dong, Y.; Xuan, S.; Zhang, Z. Controlled synthesis of crystalline and helical *n*-alkyl poly(L-alanine). *Macromolecules.* **2024**, *57* (15), 7031−7042.

https://doi.org/10.1021/acs.macromol.6c00471
Macromolecules 2026, 59, 6854−6863

(48) Lu, M.; Zhu, Z.; Wang, S.; Wang, L.; Yang, H.; Yang, Z.; Yang, L.; Gao, Y. Q.; Lu, H. Polymerization chaperone for the controlled, homogeneous synthesis of proline-based homo- and copolypeptides. *J. Am. Chem. Soc.* **2026**, *148* (11), 12033−12043.
(49) Lv, W.; Wang, Y.; Li, M.; Wang, X.; Tao, Y. Precision synthesis of polypeptides *via* living anionic ring-opening polymerization of *N*-carboxyanhydrides by tri-thiourea catalysts. *J. Am. Chem. Soc.* **2022**, *144* (51), 23622−23632.
(50) Zhao, W.; Gnanou, Y.; Hadjichristidis, N. Organocatalysis by hydrogen-bonding: a new approach to controlled/living polymerization of α-amino acid *N*-carboxyanhydrides. *Polym. Chem.* **2015**, *6* (34), 6193−6201.
(51) Li, K.; Li, Z.; Shen, Y.; Fu, X.; Chen, C.; Li, Z. Organobase 1,1,3,3-tetramethyl guanidine catalyzed rapid ring-opening polymerization of α-amino acid *N*-carboxyanhydrides adaptive to amine, alcohol and carboxyl acid initiators. *Polym. Chem.* **2022**, *13* (5), 586−591.
(52) Xu, G.; Tang, G.; Bai, H. Cyclodextrin-initiated *N*-carboxyanhydride polymerization for the design of stereostructural dobby polypeptides with jellyfish-type architecture. *Angew. Chem., Int. Ed.* **2025**, *64* (18), No. e202501058.
(53) Zheng, X.; Huang, J.; Sheng, H.; Yuan, Z.; Zhao, Y.; Liu, X.; Song, Z.; Cheng, J. Accelerated and controlled polymerization of *N*-carboxyanhydrides in the presence of tertiary amines with minimized activated monomer mechanism. *Macromolecules.* **2026**, *59* (2), 728−735.
(54) Yuan, J.; Shi, D.; Zhang, Y.; Lu, J.; Wang, L.; Chen, E.-Q.; Lu, H. 4-hydroxy-l-proline as a general platform for stereoregular aliphatic polyesters: controlled ring-opening polymerization, facile functionalization, and site-specific bioconjugation. *CCS Chem.* **2020**, *2* (5), 236−244.
(55) Kaljurand, I.; Kutt, A.; Soovali, L.; Rodima, T.; Maemets, V.; Leito, I.; Koppel, I. A. Extension of the self-consistent spectrophotometric basicity scale in acetonitrile to a full span of 28 pKa units: unification of different basicity scales. *J. Org. Chem.* **2005**, *70* (3), 1019−1028.
(56) Kütt, A.; Selberg, S.; Kaljurand, I.; Tshepelevitsh, S.; Heering, A.; Darnell, A.; Kaupmees, K.; Piirsalu, M.; Leito, I. pK_a values in organic chemistry-making maximum use of the available data. *Tetrahedron Lett.* **2018**, *59* (42), 3738−3748.
(57) Tshepelevitsh, S.; Kütt, A.; Lõkov, M.; Kaljurand, I.; Saame, J.; Heering, A.; Plieger, P. G.; Vianello, R.; Leito, I. On the basicity of organic bases in different media. *Eur. J. Org. Chem.* **2019**, *2019* (40), 6735−6748.
(58) Wang, W.; Fu, H.; Lin, Y.; Cheng, J.; Song, Z. Cooperative covalent polymerization of n-carboxyanhydrides: from kinetic studies to efficient synthesis of polypeptide materials. *Acc. Mater. Res.* **2023**, *4* (7), 604−615.
(59) Bellmaine, S.; Schnellbaecher, A.; Zimmer, A. Reactivity and degradation products of tryptophan in solution and proteins. *Free Radical Biol. Med.* **2020**, *160*, 696−718.
(60) Vivian, J. T.; Callis, P. R. Mechanisms of tryptophan fluorescence shifts in proteins. *Biophys. J.* **2001**, *80* (5), 2093−2109.
(61) Dave, D. R.; Kassem, S.; Coste, M.; Xu, L.; Tayarani-Najjaran, M.; Podbevšek, D.; Colon-De Leon, P.; Zhang, S.; Ortuno Macias, L.; Sementa, D.; Pérez-Ferreiro, M.; Ayati, N. S.; Choudhury, M. A.; Veerasammy, K.; Doganata, S.; Zhong, T.; Weng, C.; Morales, J.; Favaro, D. C.; Marianski, M.; Ahn, S. Y.; Obermeyer, A. C.; Wang, T.; Li, T.-D.; Chen, X.; Tu, R.; He, Y.; Ulijn, R. V. Adaptive peptide dispersions enable drying-induced biomolecule encapsulation. *Nat. Mater.* **2025**, *24* (9), 1465−1475.
(62) Santiveri, C. M.; Jimenez, M. A. Tryptophan residues: scarce in proteins but strong stabilizers of β-hairpin peptides. *Biopolymers.* **2010**, *94* (6), 779−790.
(63) Woody, R. W. Contributions of tryptophan side chains to the far-ultraviolet circular dichroism of proteins. *Eur. Biophys. J.* **1994**, *23* (4), 253−262.
(64) Bagheri, M.; Nikolenko, H.; Arasteh, S.; Rezaei, N.; Behzadi, M.; Dathe, M.; Hancock, R. E. W. Bacterial aggregation triggered by fibril forming tryptophan-rich sequences: effects of peptide side chain and membrane phospholipids. *ACS Appl. Mater. Interfaces.* **2020**, *12* (24), 26852−26867.
(65) Xie, X.; Moon, P. J.; Crossley, S. W. M.; Bischoff, A. J.; He, D.; Li, G.; Dao, N.; Gonzalez-Valero, A.; Reeves, A. G.; McKenna, J. M.; Elledge, S. K.; Wells, J. A.; Toste, F. D.; Chang, C. J. Oxidative cyclization reagents reveal tryptophan cation−π interactions. *Nature.* **2024**, *627* (8004), 680−687.
(66) Kumar, R.; Khan, S.; Ghosh, D.; Karras, G.; Clark, I. P.; Greetham, G. M.; Oliver, T. A. A.; Orr-Ewing, A. J.; Fielding, H. H. Dynamic equilibrium between the fluorescent state of tryptophan and its cation-electron ion pair governs triplet state population. *J. Am. Chem. Soc.* **2025**, *147* (35), 32064−32076.
(67) Song, F.; Wu, F.; Feng, W.; Tang, Z.; Giesy, J. P.; Guo, F.; Shi, D.; Liu, X.; Qin, N.; Xing, B.; Bai, Y. Fluorescence regional integration and differential fluorescence spectroscopy for analysis of structural characteristics and proton binding properties of fulvic acid subfractions. *J. Environ. Sci.* **2018**, *74*, 116−125.

https://doi.org/10.1021/acs.macromol.6c00471
Macromolecules 2026, 59, 6854−6863